arXiv:cond-mat/9405042v1 14 May 1994

Non-equilibrium dynamics in the random bond Ising chain: A reminiscence of aging in spin glasses

H. Rieger, J. Kisker and M. Schreckenberg

Institut für Theoretische Physik

Universität zu Köln

50937 Köln,Germany

(February 1, 2008)

Abstract

Results of extensive Monte-Carlo simulations that investigate the out-of-equilibrium dynamics of the one-dimensional Ising spin glass model with a Gaussian bond-distribution are presented. At low enough temperatures a typical (interrupted) aging scenario is established as in two- and similar to three-dimensional spin glass models. Since the underlying mechanism is a slow domain-growth we study in detail spatial correlations and the time-dependence of the domain- as well as kink-statistics. We find that all correlation functions in time and in space as well as the domain-size probability distribution function obey simple scaling laws.

75.10N, 75.50L, 75.40G.

Typeset using REVTEX

I. INTRODUCTION

Non-equilibrium dynamics in real spin glasses, also known as *aging*, has been a major focus of research interest of experimentalists since many years [1–3]. Quite recently, also theoreticians began to shift their attention from the equilibrium statistical mechanics [4] to the out-of-equilibrium dynamics of various spin glass models [5–12]. It has been argued that aging is a characteristic feature of the low temperature dynamics of spin glasses and it has already been established in experiments [13,14] and numerical simulations [6,15] investigating two-dimensional spin glasses (which do not posses a finite temperature phase transition) that a true spin glass phase is not a necessary prerequisite for it to be observable on suitable time-scales. The only differences remaining is then that aging is interrupted at some maximal waiting time, which is equivalent to the finite, but large, equilibration time at this temperature (see also [2] and [5]).

In this paper we will demonstrate that even in a disordered but *non-frustrated* system a very similar scenario will occur. The model we consider here is the one-dimensional Ising spin glass with a Gaussian bond-distribution, which can be mapped, simply via a gauge-transformation of the spins, onto a random, ferromagnetic Ising chain. Thus the ground state is fully magnetized and the dynamics at low temperatures is characterized by (ferromagnetic) domain-growth, which is drastically slowed down by the presence of a huge number of metastable states [16–18]. An important ingredience, however, is a continuous, unbounded bond distribution, although some of the features to be presented can be anticipated already in the one-dimensional $\pm J$ Ising spin glass model. The latter is isomorphic to the ferromagnetic Ising chain, whose non-equilibrium dynamics is exactly solvable and has been studied extensively [19–22]. Only for a continuous bond distribution one has a broad distribution of (free) energy barriers, which are responsible for the broad spectrum of relaxation times.

The paper is organized as follows: The next section reports known exact results for the autocorrelation function and the two-point correlation function of $\pm J$ Ising chain. In section 3 we present results of Monte-Carlo simulations of the random bond Ising chain, which cover correlations in time and in space. A scaling analysis along the lines sketched in

section 2 is performed and compared with the results of a recently proposed one-dimensional domain-growth model [18]. Section 4 is devoted to a domain-size and -kink statistics that we obtained from our numerical simulations and here also a scaling analysis is performed. Section 5 discusses the concept of an overlap length [20,25] in the random bond Ising chain and summarizes our findings.

II. THE $\pm J$ CHAIN

In this section we recapitulate what is known about the non-equilibrium dynamics of the $\pm J$ chain, which can be solved exactly [19–23]. On one hand we introduce in this way the quantities that we intend to study for the random bond Ising chain and on the other we shall see what kind scaling behavior can be expected for these quantities. The one-dimensional $\pm J$ Ising spin glass model (which is no spin glass at all) is defined by the Hamiltonian

$$H = -\sum_{i=1}^{N} J_i S_i S_{i+1} \ , \tag{1}$$

where $S_i = \pm 1$ are Ising spins and the bonds J_i are chosen at random from a binary distribution

$$P(J_i) = \frac{1}{2}[\delta(J_i - 1) + \delta(J_i + 1)] \ , \tag{2}$$

however, this quenched disorder can be removed (up to a negligible boundary term) via the Gauge-transformation $S_i' = S_i \prod_{k=1}^{i} \mathrm{sign}\, J_k$. Thus (1) is equivalent to the simple ferromagnetic spin chain. All results reported below are for $N \to \infty$. The dynamics is the usual Glauber-dynamics [19], where each spin is flipped with a probability

$$w(S_i \to -S_i) = \frac{1}{2}[1 - \tanh\, \beta(J_{i-1}S_{i-1} + J_i S_{i+1})\,] \ . \tag{3}$$

The corresponding Master equation leads to a time dependent probability distribution for spin configurations with which expectation values are calculated (the initial distribution is uniform, i.e. the at $t = 0$ all spin are chosen at random). Such a quantity for instance is the autocorrelation function [19]

$$C(t, t_w) = \langle S_i(t_w) S_i(t + t_w) \rangle \ , \tag{4}$$

which will be studied numerically for the random bond chain in the next section. At $T = 0$ one obtains [19,21]

$$C(t, t_w) = \frac{2}{\pi} \text{arc sin} \left\{ 1 + \frac{1}{2} \frac{t}{t_w} \right\}^{-1/2} \quad . \tag{5}$$

Note that $C(t, t_w)$ is a function of t/t_w only and such a scaling behavior has been reported for the same quantity in various other spin glass models [5,7,9,11,15]. For illustration and comparison with these models we have depicted in figure 1 a plot of $C(t, t_w)$ for various waiting times. Furthermore one gets for short and for long times

$$C(t, t_w) \quad \approx \quad \begin{cases} 1 \, - \, \frac{2}{\pi} \, (t/t_w)^{1/2} & \text{for} \quad t \ll t_w \ , \\ \frac{\sqrt{8}}{\pi} \, (t/t_w)^{-1/2} & \text{for} \quad t \gg t_w \ . \end{cases} \tag{6}$$

For $T > 0$ the time-dependence of $C(t, t_w)$ is determined by the correlation length (which is infinite for $T = 0$), which we consider now. Spatial correlations are defined by

$$G_T(r, t_w) = \langle S_i(t_w) S_{i+r}(t_w) \rangle \ . \tag{7}$$

For $t_w \to \infty$ one has

$$\lim_{t_w \to \infty} G_T(r, t_w) = G_T^{\text{eq}}(r) = \{ \tanh(\beta J) \}^r \tag{8}$$

which defines the equilibrium correlation length $\xi_{T,\text{eq}}$ via $\xi_{T,\text{eq}}^{-1} = -\log\{\tanh(\beta J)\}$ [19]. It can be shown [21] that for $1 \ll t_w \ll \xi_{T,\text{eq}}^2$

$$G_T(r, t_w) = \tilde{g} \left(\frac{r}{\xi_T(t_w)} \right) \ , \tag{9}$$

where the characteristic length scale grows like

$$\xi_T(t_w) \propto \sqrt{t_w} \tag{10}$$

until it saturates for $t_w \to \xi_{T,\text{eq}}^2$ and one recovers $G_T(r, t_w) \to G_T^{\text{eq}}(r)$. Similarly, for $1 \ll t_w \ll \xi_{T,\text{eq}}$ one would expect instead of (5)

$$C_T(t, t_w) = \tilde{c}_T \left(\frac{t}{\tau(T, t_w)} \right) \ , \tag{11}$$

where the characteristic time scale grows like $\tau(T, t_w) \sim t_w$ for small temperatures, but saturates at $\xi_{\text{eq}}^2(T)$. All the above results are very reminiscent of characteristic aging phenomena observed in other spin glass models. The main difference to these much more

complex models lies in the waiting time dependence of the correlation length $\xi_T(t_w)$, which predicts a rather *fast* domain growth, which makes it hard to observe them on macroscopic time scales at non-zero temperatures. Furthermore, a significantly different scaling behavior for e.g. $C(t, t_w)$ will be present in systems that are characterized by activated dynamics and logarithmic domain growth [25].

III. THE RANDOM BOND ISING CHAIN

The random bond Ising chain is defined in the same as the $\pm J$ Ising chain discussed in the last section up to a different bond-distribution: Instead of (2) we consider here the Gaussian distribution of the random bonds

$$P(J_i) = \frac{1}{\sqrt{2\pi}} \exp\left(-\frac{J_i^2}{2}\right) , \tag{12}$$

(see e.g. [24] for the corresponding spin glass model in higher dimensions). As before one can remove all minus-signs in the bonds by a gauge-transformation that leads to a purely ferromagnetic bond distribution $\tilde{P}(J_i) = 2P(J_i)\theta(J_i)$.

We performed Monte-Carlo simulations of the single-spin-flip Glauber dynamics (3) with typical chain lengths of $N = 10000$ (imposing periodic boundary conditions) and averaged over 128 to 512 samples, i.e. realizations of the disorder. Since we performed our simulations on a Parsytec GCel1024 parallel computer, using up to 256 different processors. We constrained the system size to fit one system into the memory of one T805-transputer in order to avoid communication delays. Alternatively we also could have made a few runs for chain-lengths of 10^6–10^7 and distribute chain-segments over several processors, however, by varying the system size, we checked that our date were not spoiled by finite-size effects.

The correlation functions (4) and (7) have to be averaged over the quenched disorder. In addition, in order to obtain better statistics we calculated instead of single-site/single-time quantities, appropriate space and time averages as

$$C(t, t_w) = \frac{1}{N}\sum_{i=1}^{N} \frac{1}{\Delta t + 1} \sum_{t'=t}^{t+\Delta t} [S_i(t' + t_w)S_i(t_w)]_{\text{av}} , \tag{13}$$

$$G(r, t_w) = \frac{1}{N}\sum_{i=1}^{N} \frac{1}{\Delta t + 1} \sum_{t'=t}^{t+\Delta t} [S_i(t' + t_w)S_{i+r}(t' + t_w)]_{\text{av}} , \tag{14}$$

with suitable values for the time-window Δt ($1 \leq \Delta t \ll t$) and $[\cdots]_{\rm av}$ indicating the disorder average. If taken literally the expectation values in (4) and (7) should be obtained via different realizations of the thermal noise. However, we checked that in using (13,14) we get the same results.

In figure 2 we show our results for $C(t, t_w)$ at different temperatures. The picture is equivalent to that obtained for the same quantity in the two-dimensional Ising spin-glass [15] and, at low temperatures, reminiscent of the three-dimensional spin glass model [7] and the SK-model within the spin glass phase [11]. This is what we would like to call interrupted aging as been observed experimentally in charge-density wave systems [2]. At higher temperatures the curves collapse for larger waiting times t_w, which means that the system is equilibrated. The waiting time at which this happens is the equilibration time $\tau_{\rm eq}$. At lower temperatures this time scale is out of reach for the amount of CPU time that is available to us, hence all curves seem to be shifted logarithmically on the time axes by t_w.

Similar to what has been observed in other spin glass models [5,7,9,11,15] we established the scaling

$$C(t, t_w) = \tilde{c}_T \left(\frac{t}{\tau(T, t_w)} \right) , \tag{15}$$

A scaling plot of this kind is depicted in figure 3, where the insert shows the characteristic time-scale $\tau(T, t_w)$. For small waiting times at low temperatures it is, as expected, $\tau(T, t_w) \approx t_w$, and it saturates for increasing t_w at $\tau(T, t_w) = \tau_{\rm eq}(T)$.

Next we turn our attention to the spatial two-point correlation function (7). The (averaged) equilibrium correlation function can easily be determined exactly as

$$G_{\rm eq}(r) = [\tanh(\beta J)]^r_{\rm av} \tag{16}$$

(for a discussion about the differences between averaged and typical or most probable values of the spatial correlations in this system see [26]) which yields an equilibrium correlation length

$$\xi^{-1}_{\rm eq}(T) = -\log [\tanh(\beta J)]_{\rm av} \propto T \quad \text{for T} \ll 1 \, . \tag{17}$$

The non-equilibrium spatial correlation function $G_T(r, t_w)$, defined in (7) respectively (14), will approach (16) at waiting times t_w larger than the equilibration time $\tau_{\rm eq}(T)$. This is

shown in figure 4 for two different temperatures, where at $T = 0.4$ one observes indeed this data-collapse. The curves are approximate straight lines in a linear-log plot, which means that the spatial correlations decay exponentially with a characteristic length scale $\tilde{\xi}_T(t_w)$. This length is roughly equal to the length scale $\sigma_T(t_w)$ that yields a good data-collapse for a scaling plot according to equation (9), i.e.

$$G(r, t_w) = \tilde{g}(r/\sigma(t_w)) \; , \tag{18}$$

which is shown in figure 5. The smoothest curve for the waiting-time dependent length scale can be obtained via the introduction of the (effective) correlation length

$$\xi_T(t_w) = \int_0^\infty dr \, G_T(r, t_w) \; , \tag{19}$$

note, however, that for any t_w and T we have $\xi_T(t_w) \approx \sigma_T(t_w) \approx \tilde{\xi}_T(t_w)$. The correlation length $\xi_T(t_w)$ is shown in the insert of figure 5 within a log-log plot, where one observes that this length scale grows much slower than in the $\pm J$ chain, cf. (10). Similar to what has been found in the two-dimensional spin glass model [15] it seems that (see the curve for $T = 0.2$) $\xi_T(t_w)$ grows algebraically as

$$\xi_T(t_w) \propto t_w^{\alpha(T)} \qquad \text{for} \quad t_w \ll \tau_{\rm eq} \; , \tag{20}$$

with a small, temperature-dependent exponent $\alpha(T)$ (note that $\lim_{t_w \to \infty} \xi_T(t_w) = \xi_T^{\rm eq}(t_w)$, so that again).

The remanent magnetiziation $M_{\rm rem}(t) = C(t, 0)$ decreases with increasing domain-size. If one assumes $M_{\rm rem}(t) \propto \xi_T(t_w)^{-\lambda}$) as for instance in [25], one obtains with (20) an algebraic decay $M_{\rm rem}(t) \propto t^{-a(T)}$ as long as $\xi_T(t_w) \ll \xi_{rmeq}(T)$, which would concur with the prediction [16]. However, we find that the time dependence of the remanent magnetization can be better fitted to a stretched exponential, similar to the lower bound given in in [17].

Starting from a one-dimensional domain growth model the exact scaling function for the two-point correlations has been predicted in [18]. It is (for an unbounded bond-distribution) $G(r, t_w) = \overline{c}(r/L_T(t_w))$ (similar to (9)) with

$$\overline{c}(x) = \int_0^1 dy \, 2y^2 \exp(-2x/y) \log(y/(1-y)) \tag{21}$$

and $L_T(t_w)$ the average domain-size after a waiting time t_w at temperature T. Note that $\overline{c}(x) \approx \exp(-2.19\,x)$ for $x \in [0, 10]$ to great precision. By rescaling the variable x in (21) by a factor of roughly one half one gets a good agreement with our data, as is shown in figure 5. This means that the free parameter L_0 in [18], which is identified with the average domain-size, is approximately twice as large as our correlation-length $L_0 \approx 2\xi_T(t_w)$. Note that due to the construction of the model [18] no prediction about the time dependence of this length scale could be made.

IV. DOMAIN-STATISTICS

The slow domain growth in spin glasses in general [25,27] and in the random bond Ising chain in particular [16,17,20] is the reason for their glassy dynamics. This fact has already been established numerically for instance in the site-diluted Ising model [28], the random field Ising model [29] and the random bond ferromagnetic Ising model [30] in two dimensions. In contrast to the $\pm J$ chain, where this slow dynamics is appropriately described by simple kink-diffusion and -annihilation [22] (which is also the ultimate reason for the "random-walk-result" (10)), the quenched randomness gives rise to a huge number of metastable states and (free) energy barriers of all sizes. Thus the mechanism of domain growth in the presence of disorder is significantly modified and slowed down. However, it is still describable by means of diffusion and annihilation of kinks (broken bonds) in a random potential [16]. Nevertheless it has not been possible up to now to derive an analytically exact expression for the average domain-size as a function of the waiting time.

We calculated the time-dependent domain-size distribution during our Monte-Carlo simulations in the following way (note that this definition of domains is different from the cluster-definition given in [31]) : By recording the time averaged local magnetizations

$$m_i(t_w) = \frac{1}{t_w} \sum_{t=t_w}^{2t_w-1} S_i(t) \tag{22}$$

for each sample we identified domains as connected segments of the chain in which all local magnetizations have the same sign. The length of one domain is just the size of one segment. Then we determine the number n_l of domains of length l in all samples ($\sigma = \sum_l n_l = N \cdot \mathcal{S}$,

N =system size, $\mathcal{S}$ = number of samples) and get the probability $P(l, t_w)$ for a spin to be within a domain of length l via

$$P_T(l, t_w) = l\, n_l(t_w) \,/\, \Sigma \,. \tag{23}$$

In figure 6 we depict the result for two different temperatures. According to the scaling behavior found in the last section the probability distribution for the domain-size should scale in a similar way

$$P_T(l, t_w) \approx \frac{1}{L_T(t_w)}\, \tilde{p}\, \left(\frac{l}{L_T(t_w)} \right) \,, \tag{24}$$

An appropriate choice for $L_T(t_w)$ is the mean value or average domain-size $L(t_w) = \int dl\, l\, P_T(l, t_w)$, a scaling plot is shown in figure 7 and the insert shows $L_T(t_w)$ as a function of the waiting time. The shape of the curve is similar to that of $\xi_T(t_w)$, although the average domain-size is much larger than the correlation length. This is due to the definition of domains that we have chosen: It is only the sign and not the magnitude of the local magnetizations that determines whether a spin belongs to a domain or not. If a spin has a rather small magnetization during a time interval of length t_w (which means that it has been dynamically "active" rather than frozen) it contributes only marginally to the correlation function, but fully to our domain-size. Therefore both quantities are expected to be related to each other, but are not equal.

It is worth stressing that $P_T(l, t_w)$ is not Gaussian and that the average $L_T(t_w)$ is dominated by the long tail of the domain-size distribution. The typical domain-size, which is defined by the length l, where $P_T(l, t_w)$ attains its maximum, is much smaller than the average $L_T(t_w)$, however, it depends on the waiting time in the same way as the average (different from what has been observed in the random field Ising chain in a transverse field [32]).

The number of kinks $N_K(t_w)$ in the system, i.e. bonds between spins that are anti-parallel, is connected to the average domain length via $L_T(t_w) = N/N_K(t_w)$. By inspecting the probability distribution $K_T(J, t_w)$ for the kink-strength J one obtains information about the thermal energy of the chain. The ground state energy per spin of the system is given by $E_0 = -\int_0^\infty dJ\, P(J)$, for non-zero temperatures (and for all waiting times t_w) broken

bonds will increase the thermal energy by an amount $\Delta E_T(t_w) = \int_0^\infty dJ\, J\, K_T(J, t_w)$. In figure 8 we show the kink-strength distribution $K_T(J, t_w)$ for two temperatures. We note that, comparing it for $T = 0.4$ with figure 6, the kink-strength distribution seems to reach stationarity (i.e. independence of t_w) much faster than the domain-size distribution. Since the latter yields information about the magnetization of the system, this is in full agreement with [16], where it has already been noted, that the relaxation of the thermal energy is much faster than that of the magnetization. The whole kink-strength distribution scales nicely with the characteristic energy scale $\delta E_T(t_w)$:

$$K_T(J, t_w) = \frac{1}{\Delta E_T(t_w)} \tilde{k} \left(\frac{J}{\Delta E_T(t_w)} \right) , \tag{25}$$

as is shown in figure 9. The insert shows the waiting time dependence of the excess energy $\Delta E_T(t_w)$ in a log-log plot, indicating an algebraic decay over the range of time-scales considered (note that it has to saturate at a non-vanishing value for non-zero temperatures, which means that an algebraic decay cannot hold forever). This is in agreement with what has been proposed in [16].

V. DISCUSSION

Before summarizing our results we want to discuss the issue of an overlap length [20,25,27] in the random bond Ising chain. It has been found that the spin-glass state is extremely sensitive to temperature- or field changes by an infinitesimal amount [33]. This sensitivity is observable via the overlap correlation function

$$\begin{aligned} K_{T,H,\Delta T,\Delta h}(r) &= [\langle S_i S_{i+r} \rangle^{\rm eq}_{T,h} \langle S_i S_{i+r} \rangle^{\rm eq}_{T \pm \Delta T, H \pm \Delta h}]_{\rm av} \\ &\propto \exp\{-r/\lambda_{T,h}(\Delta T, \Delta h)\} , \end{aligned} \tag{26}$$

where the length scale $\lambda(\Delta T, \Delta h)$ is the so called overlap length. For a system with a finite correlation-length at temperature T and field-strength h, e.g. two-dimensional spin glasses or the random bond Ising chain, this is a quite trivial observation. For instance in the $\pm J$ chain at $h = \Delta h = 0$ (see section 2) it easy to see that

$$\lambda_T(\Delta T) = \{ |\log \tanh [J/T]| + |\tanh [J/(T + \Delta T)]| \}^{-1} . \tag{27}$$

The nontrivial implication of (26) is that it is expected to hold also *within* the spin glass phase of a true (e.g. higher-dimensional) spin glass, where the correlation-length is infinite [25,27,34]. The reason is a full rearrangement of the minima of the free energy on length scales larger than λ by changing the external parameters like T or h only slightly. In [25] such a scenario has been introduced artificially (however, motivated by renormalization arguments) into the $\pm J$ chain via an explicit, stochastic temperature dependence of the bonds J_i.

In the one-dimensional spin glass model such a rearrangement of the minimum-energy spin-configurations can be observed at zero temperature (where the correlation length is indeed infinite) for a situation, in which one switches on a small external field of strength Δh [16]. In the presence of a field the ground state of the chain is fragmented into segments, in which all spins are aligned with one of the two possible configurations with minimal energy at zero-field. In this process weak bonds have to be broken and field energy can be gained and thus a new length scale λ emerges. It can be shown [16] that the length of these segments, or the domain-size, depends on Δh via

$$\lambda(\Delta h) \propto \Delta h^{2/3} \, , \tag{28}$$

which can be identified with the overlap length (26) for this particular situation $T = 0, h = 0$. At finite temperatures the situation remains similar for small field changes [16]. Furthermore a generalization of the static overlap-correlation function to a non-equilibrium situation is straightforward (see [20]), but has not been investigated yet — neither numerically nor analytically.

In conclusion we have presented a detailed numerical study of the non-equilibrium dynamics of the random bond Ising chain. We have shown that many of the aging phenomena reported in the literature — as for instance strong memory effects, t/t_w scaling of the autocorrelation function and slow domain growth — can also be found in this non-frustrated model and also, although less pronounced, in pure Ising models (see section 2, and also [36], where a similar scaling of the autocorelation function as in (11) has been derived within an ε-expansion around four dimensions in a field theory for the non-equilibrium dynamics of ferromagnets).

We established simple scaling of the two-point correlation function and showed that the corresponding (temperature-independent) scaling function concurs with that proposed very recently in a one-dimensional domain-growth model [18]. In addition we have obtained the explicit time dependence of the characteristic length scale. Also the domain-size distribution and the kink-strength distribution exhibits simple scaling with an average domain size and excess energy, respectively. The time dependence of the latter quantities is algebraic as long as equilibration is not achieved, which is very reminiscent of what has been observed in higher dimensional spin glass models [7,15].

Probably most people will agree that there is an essential difference between the simple, albeit disordered, model considered here and other spin glass models — as for instance the two– and three-dimensional Edwards-Anderson model and the Sherrington-Kirkpatrick model. Apart from the presence of frustration the most significant feature of the latter, as compared to the random bond Ising chain, is the occurrence of replica symmetry breaking. It seems that this equilibrium feature of the SK-model has also interesting consequences for the non-equilibrium dynamics [8,10]. Nothing of this will ever be observed in the random bond Ising chain. However, many experimental observations on real spin glasses are reminiscent of what we have reported here. Thus, as has already been noted in [20], it seems to us to be very useful to look closer into one-dimensional models to catch some of the physics in three dimensions.

VI. ACKNOWLEDGEMENT

We would like to thank the Center of Parallel Computing (ZPR) in Köln for the generous allocation of computing time on the transputer cluster Parsytec–GCel1024. This work was performed within the SFB 341 Köln–Aachen–Jülich.

REFERENCES

[1] For an overview see e.g. M. Ledermann, R. Orbach, J. M. Hammann, M. Ocio and E. Vincent, Phys. Rev. B **44**, 7403 (1991); E. Vincent, J. Hammann and M. Ocio, chapter 7 (p. 207–236) of *Recent Progress in Random Magnets*, D. H. Ryan editor, World Scient., Singapore 1992.

[2] K. Biljakovic, J. C. Lasjaunias, P. Monceau and F. Levy, Phys. Rev. Lett. **62**, 1512 (1989) and ibid. **67**, 1902 (1991).

[3] C. Rossel, Y. Maeno and I. Morgenstern, Phys. Rev. Lett. **62**, 681 (1989).

[4] For a review of spin glasses see K. Binder and A. P. Young, Rev. Mod. Phys. **58**, 801 (1986).

[5] J. P. Bouchaud, J. Physique I **2**, 1705 (1992); J. P. Bouchaud, E. Vincent and J. Hammann, J. Physique I **4**, 139 (1994).

[6] J. O. Andersson, J. Mattson and P. Svedlindh, Phys. Rev. B **46**, 8297 (1992).

[7] H. Rieger, J. Phys. A **26**, L615 (1993); and to be published.

[8] L. Cugliandolo and J. Kurchan, Phys. Rev. Lett. **71**, 173 (1993); preprint cond-mat/9311016.

[9] G. Parisi and E. Marinari, J. Phys. A **26**, L1149 (1993).

[10] M. Mézard and S. Franz, Europhys. Lett. **26**, 209 (1994).

[11] L. Cugliandolo, J. Kurchan and F. Ritort, Phys. Rev. B **49**, 6331 (1994).

[12] H. Rieger, J. Physique I **4**, 1 (1994).

[13] J. Mattson, C. Djurberg, P. Nordblad, L Hoines, R. Stubi and J. A. Cowen, Phys. Rev. B **47**, 14626 (1993).

[14] A. Schins, A. F. M. Arts and H. W. de Wijn, Phys. Rev. Lett. **70**, 2340 (1993); A. Schins, E. M. Dons, A. F. M. Arts, H. W. de Wijn, E. Vincent, L. Leylekian and J. Hammann, Phys. Rev. B **48**, 16524 (1993).

[15] H. Rieger, B. Steckemetz and M. Schreckenberg, cond-mat/9404082 (1994).

[16] H. H. Chen and S. Ma, J. Stat. Phys. **29**, 717 (1982).

[17] S. G. W. Colborne, J. Phys. C **19**, 3669 (1986).

[18] R. E. Blundell and A. J. Bray, J. Phys. A **26**, 5237 (1993).

[19] R. J. Glauber, J. Math. Phys. **4**, 294 (1963).

[20] G. J. M. Koper and H. J. Hilhorst, Physica A, **155**, 431 (1988).

[21] A. J. Bray, J. Phys. A **22**, L67 (1989).

[22] J. G. Amar and F. Family, Phys. Rev. A **41**, 3258 (1990).

[23] M. Schreckenberg and H. Rieger, Z. Phys. B **86**, 443 (1992).

[24] R. N. Bhatt and A. P. Young, Phys. Rev. B **37**, 5606 (1988).

[25] D. S. Fisher and D. A. Huse, Phys. Rev. B **38**, 373 (1988) and ibid. **38**, 386 (1988).

[26] B. Derrida and H. Hilhorst, J. Phys. C **14**, L539 (1981).

[27] G. J. M. Koper and H. J. Hilhorst, J. Phys. France **49**, 429 (1988).

[28] G. S. Grest and D. Srolovitz, Phys. Rev. B **32**, 3014 (1985); D. Chowdhury and D. Stauffer, Z. Phys. B **60**, 249 (1985); D. Chowdhury, M. Grant and J. D. Gunton, Phys. Rev. B **35**, 6792 (1987).

[29] E. T. Gawlinsky, S. Kumar, M. Grant, J. D. Gunton and K. Kaski, Phys. Rev. B **32**, 1575 (1985); Grest, C. M. Soukoulis and K. Levin, Phys. Rev. B **33**, 7659 (1986).

[30] J. H. Oh and D. Choi, Phys. Rev. B **33**, 3448 (1986).

[31] A. Coniglio and W. Klein, J. Phys. A **13**, 2775 (1980).

[32] D. S. Fisher, Phys. Rev. Lett. **69**, 534 (1993).

[33] A. J. Bray and M. A. Moore, Phys. Rev. Lett. **58**, 57 (1987).

[34] F. Ritort, preprint cond-mat/9404020 (1994).

[35] E. Gardner and B. Derrida, J. Stat. Phys. **39**, 367 (1985).

[36] H. K. Janssen, B. Schaub and B. Schmittmann, Z. Phys. B **73**, 529 (1989).

FIGURES

FIG. 1. The autocorrelation function $C(t, t_w)$ for the $\pm J$ Ising chain at zero temperature, obtained from the exact result (5).

FIG. 2. Autocorrelation function $C(t, t_w)$ at different temperatures.

FIG. 3. Scaling plot of $C(t, t_w)$ versus $t/\tau_T(t_w)$ at temperature $T = 0.1$. the insert shows the characteristic time-scale $\tau_T(t_w)$ in a log-log plot

FIG. 4. Two-point correlation function $G_T(r, t_w)$ for different temperatures ($T = 0.2$ left and $T = 0.4$ right)

FIG. 5. Scaling-plot of $G_T(r, t_w)$ versus $r/\xi_T(t_w)$ for $T = 0.4$. The full line is the theoretical prediction scaled with a factor 0.46 (see text). The corresponding scaling plot for $T = 0.4$ yields an identical scaling function. The insert shows the correlation length $\xi_T(t_w)$ in a log-log plot.

FIG. 6. Domain-size distribution function $P_T(l, t_w)$ for different temperatures($T = 0.2$ left and $T = 0.4$ right).

FIG. 7. Scaling-plot of $P_T(l, t_w)$ versus $L_T(t_w)$ at $T = 0.2$. The insert shows the average domain-size $L_T(t_w)$ in a log-log plot. The corresponding scaling plot for $T = 0.4$ yields an identical scaling function.

FIG. 8. Kink-strength distribution $K_T(J, t_w)$ for different temperatures ($T = 0.2$ left and $T = 0.4$ right).

FIG. 9. Scaling-plot of $K_T(j, t_w)$ versus $\Delta E_T(t_w)$ for $T = 0.2$. The insert shows $\Delta E_T(t_w)$ in dependence of t_w in a log-log plot. The corresponding scaling plot for $T = 0.4$ yields an identical scaling function.

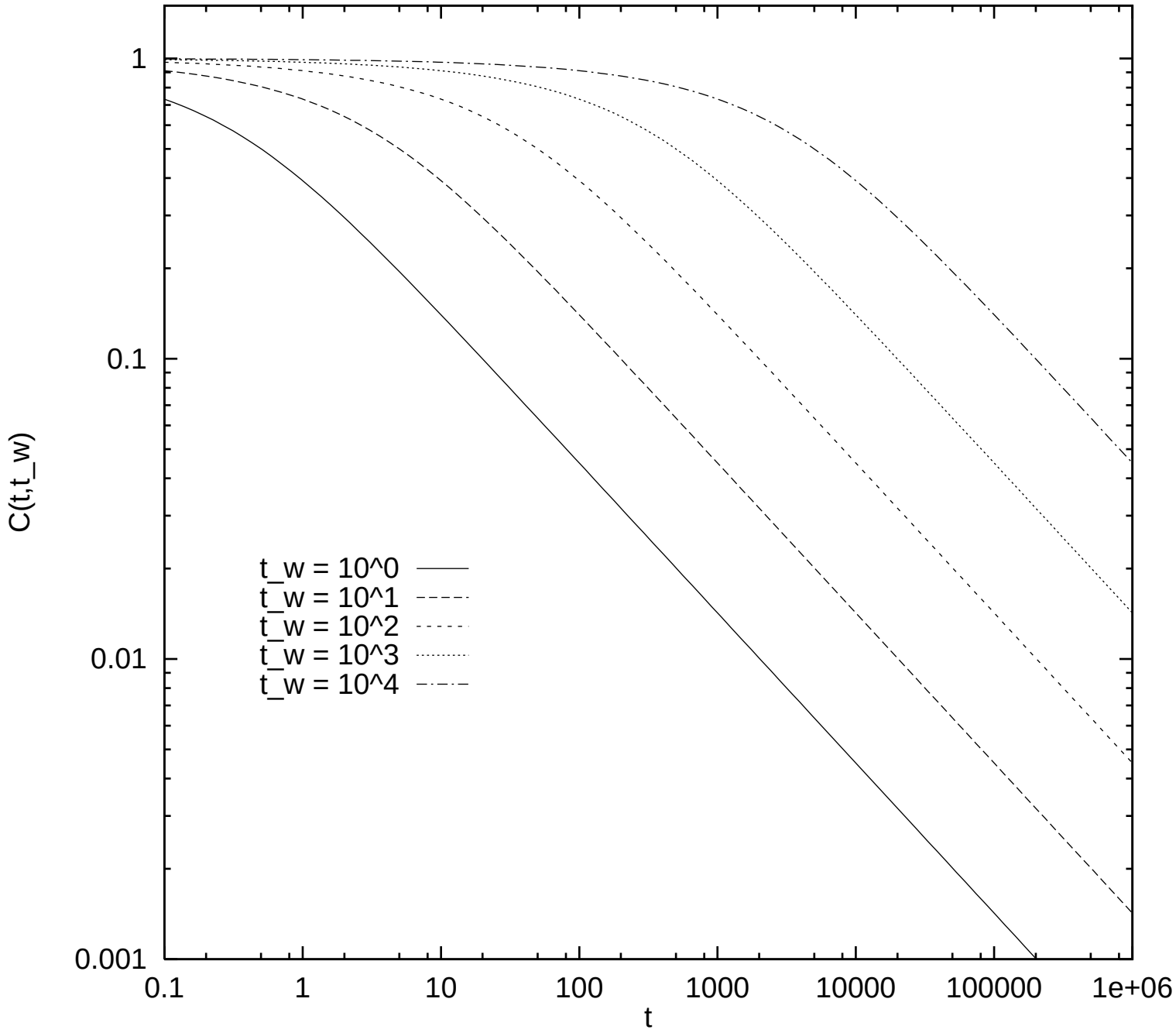
1
0.1
0.01
0.001
C(t,t_w)
0.1
1
10
100
1000
10000
100000
1e+06
t
t_w = 10^0
t_w = 10^1
t_w = 10^2
t_w = 10^3
t_w = 10^4

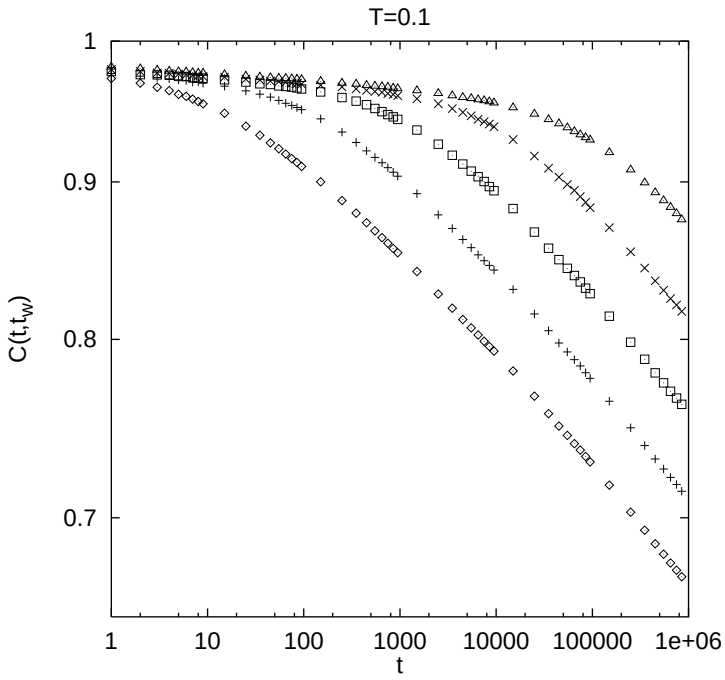
T=0.1
C(t,t_w)
t
1
0.9
0.8
0.7
1
10
100
1000
10000
100000
1e+06

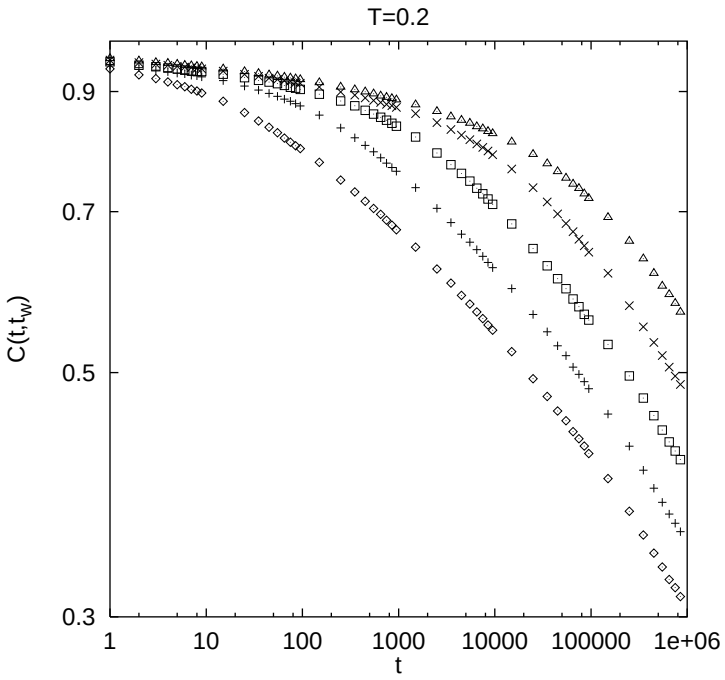
T=0.2
C(t,t_w)
t
0.9
0.7
0.5
0.3
1
10
100
1000
10000
100000
1e+06

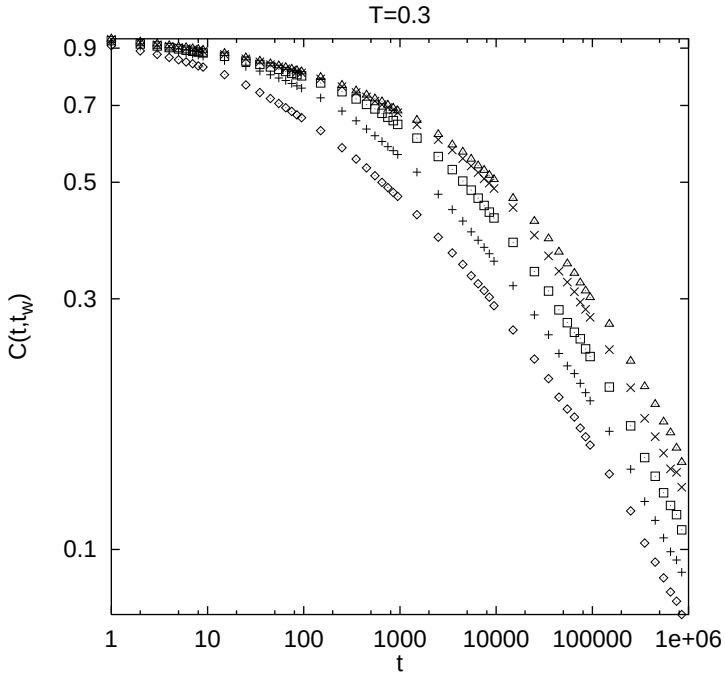
T=0.3
C(t,t_w)
t
0.9
0.7
0.5
0.3
0.1
1
10
100
1000
10000
100000
1e+06

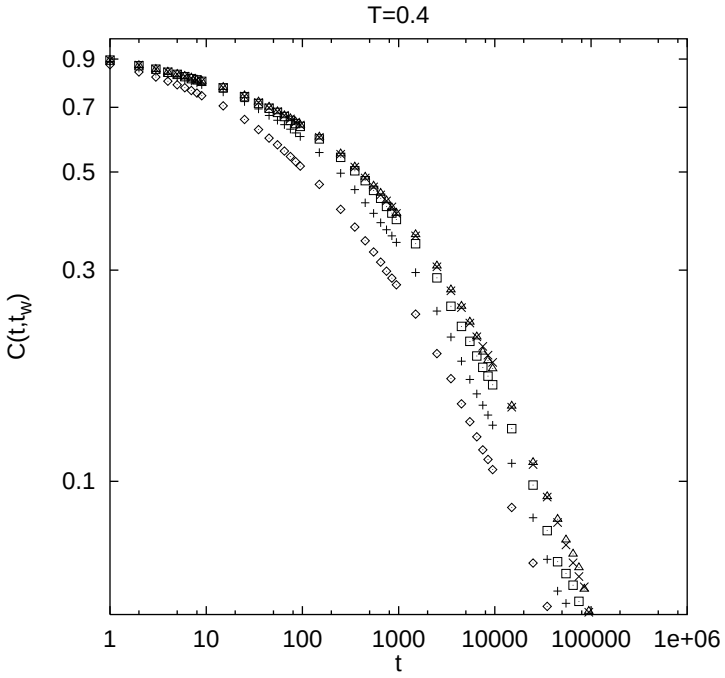
T=0.4
C(t,t_w)
t
0.9
0.7
0.5
0.3
0.1
1
10
100
1000
10000
100000
1e+06

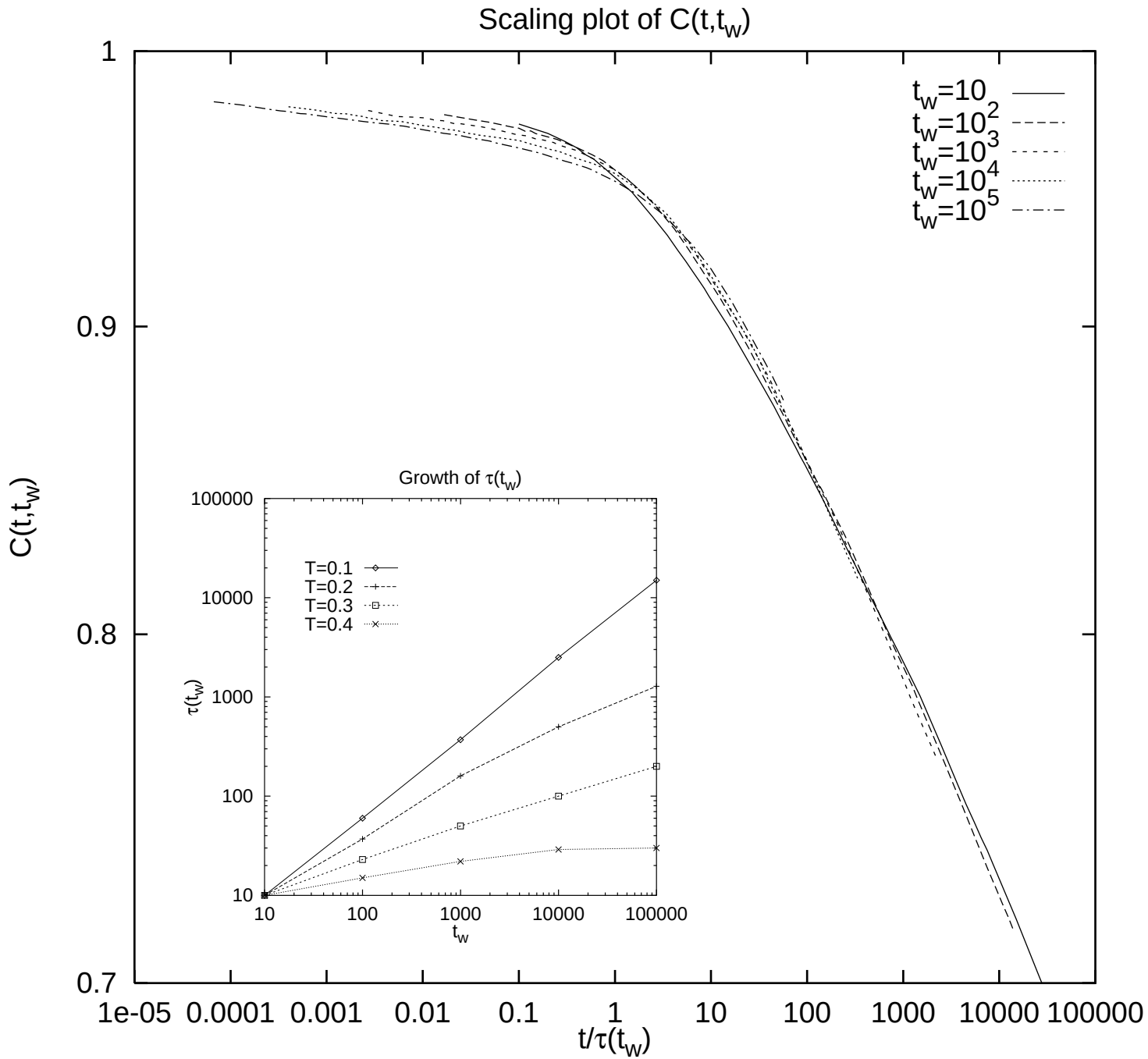
Scaling plot of C(t,t_w)
C(t,t_w)
t/τ(t_w)
1
0.9
0.8
0.7
1e-05
0.0001
0.001
0.01
0.1
1
10
100
1000
10000
100000
t_w=10
t_w=10^2
t_w=10^3
t_w=10^4
t_w=10^5
Growth of τ(t_w)
τ(t_w)
t_w
T=0.1
T=0.2
T=0.3
T=0.4
100000
10000
1000
100
10
10
100
1000
10000
100000

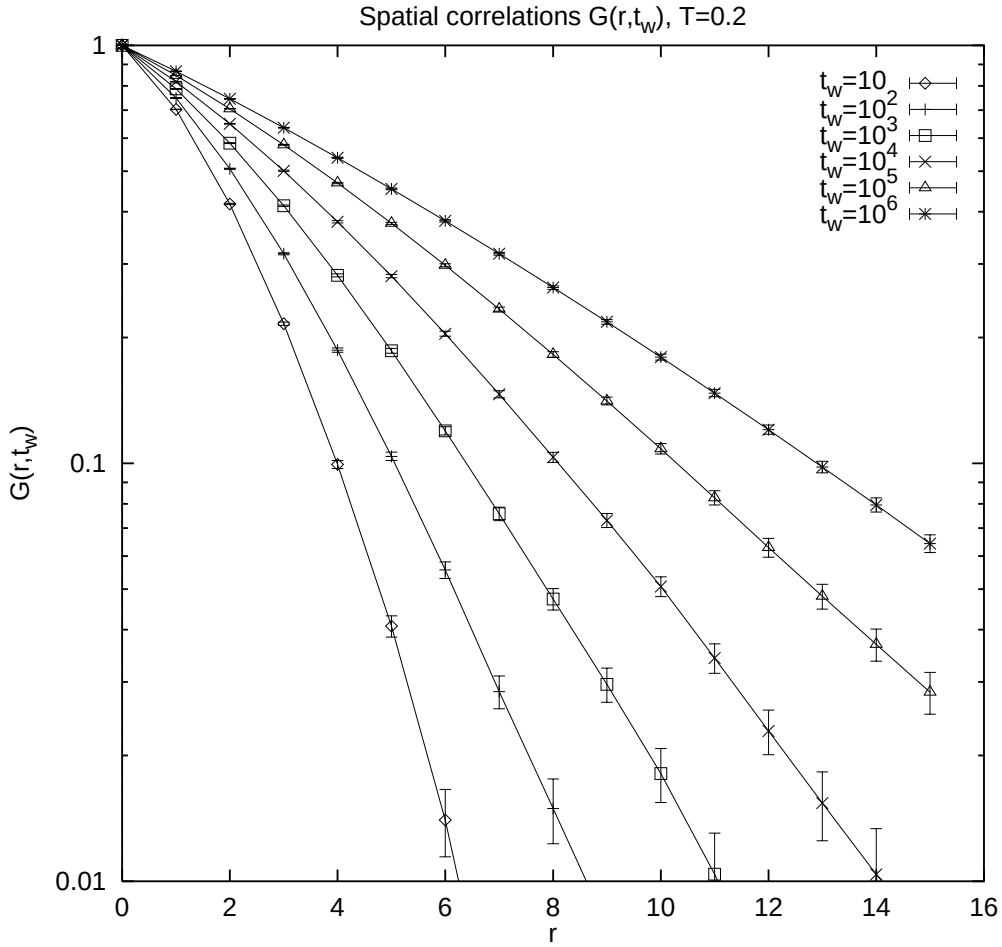
Spatial correlations G(r,t_w), T=0.2
G(r,t_w)
r
1
0.1
0.01
0
2
4
6
8
10
12
14
16
t_w=10
t_w=10^2
t_w=10^3
t_w=10^4
t_w=10^5
t_w=10^6

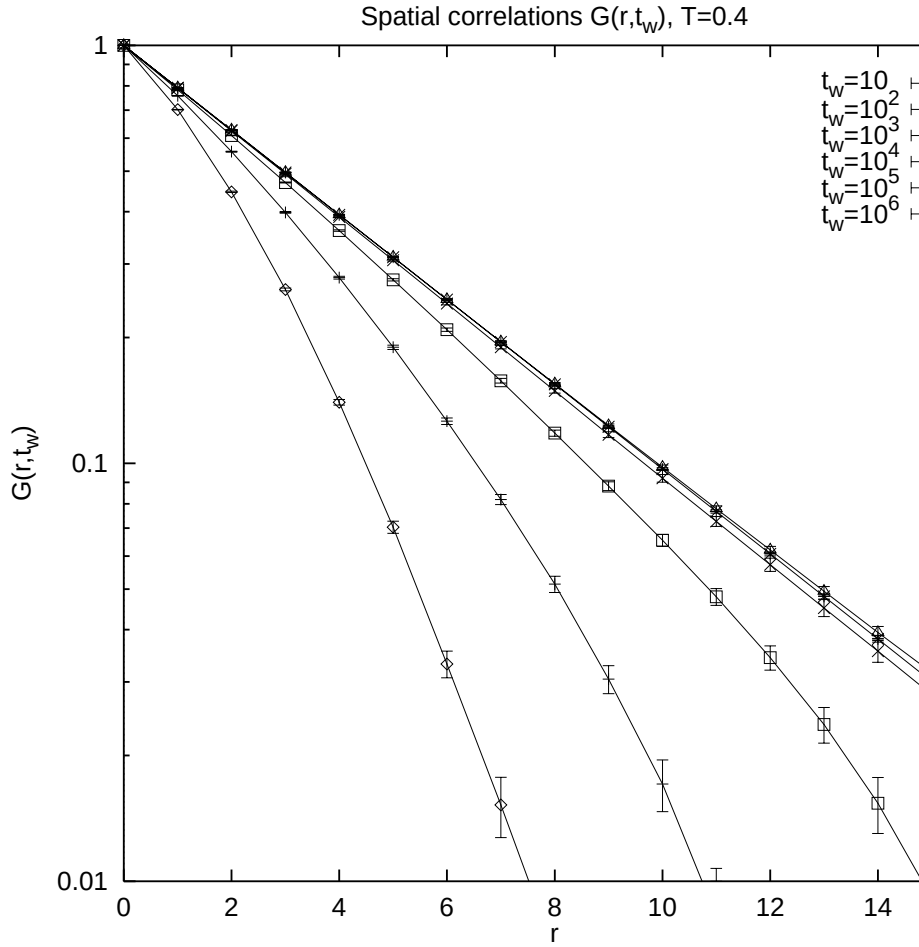
Spatial correlations G(r,t_w), T=0.4
G(r,t_w)
r
1
0.1
0.01
0
2
4
6
8
10
12
14
t_w=10
t_w=10^2
t_w=10^3
t_w=10^4
t_w=10^5
t_w=10^6

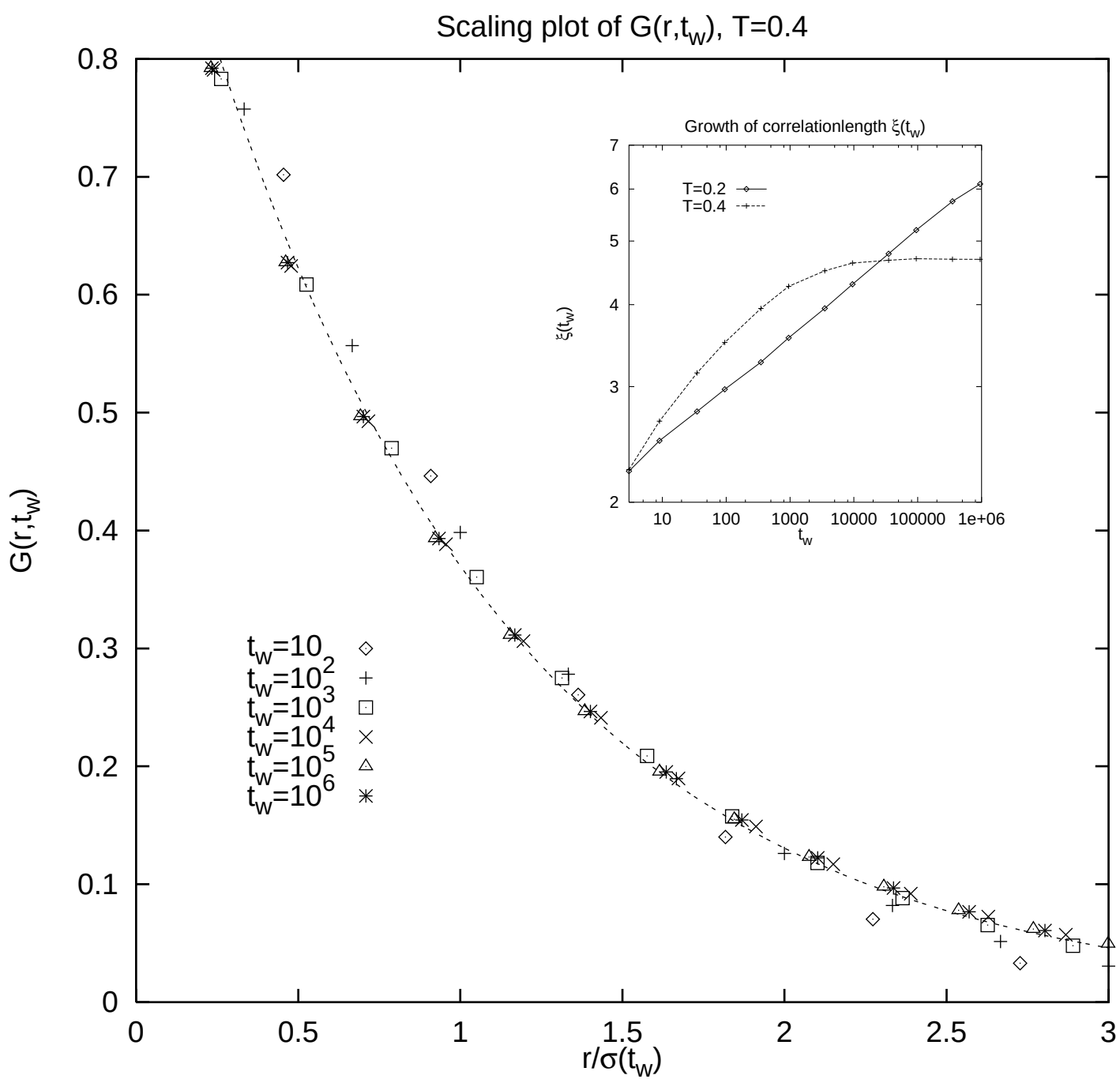
Scaling plot of G(r,t_w), T=0.4
G(r,t_w)
r/σ(t_w)
0
0.1
0.2
0.3
0.4
0.5
0.6
0.7
0.8
0
0.5
1
1.5
2
2.5
3
t_w=10
t_w=10^2
t_w=10^3
t_w=10^4
t_w=10^5
t_w=10^6
Growth of correlationlength ξ(t_w)
ξ(t_w)
t_w
T=0.2
T=0.4
2
3
4
5
6
7
10
100
1000
10000
100000
1e+06

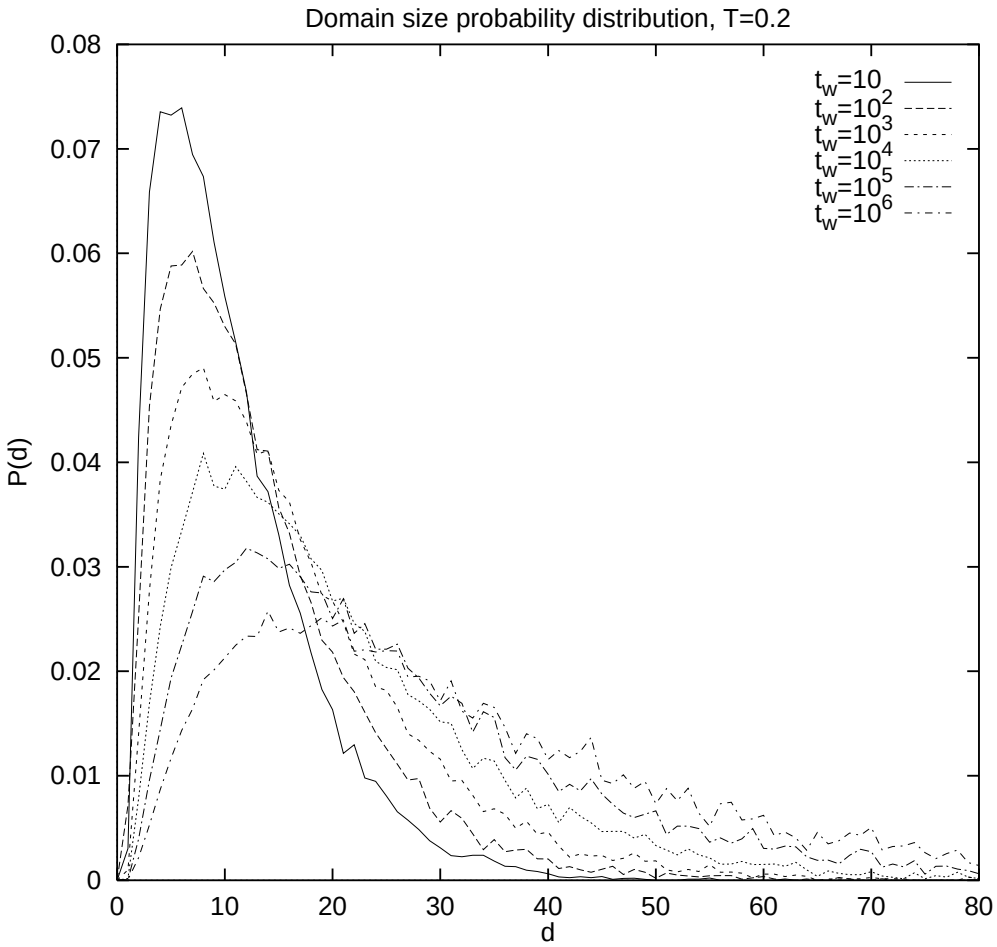
Domain size probability distribution, T=0.2
P(d)
d
0.08
0.07
0.06
0.05
0.04
0.03
0.02
0.01
0
0
10
20
30
40
50
60
70
80
$t_w=10$
$t_w=10^2$
$t_w=10^3$
$t_w=10^4$
$t_w=10^5$
$t_w=10^6$

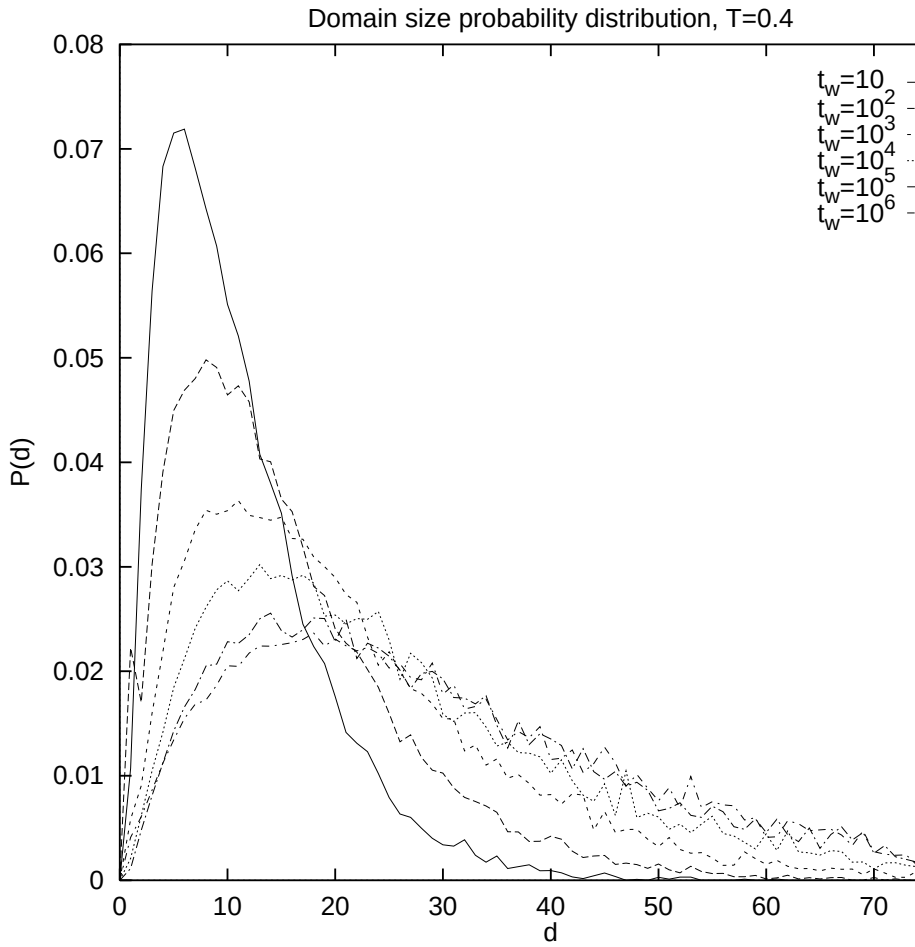
Domain size probability distribution, T=0.4
P(d)
d
0.08
0.07
0.06
0.05
0.04
0.03
0.02
0.01
0
0
10
20
30
40
50
60
70
$t_w=10$
$t_w=10^2$
$t_w=10^3$
$t_w=10^4$
$t_w=10^5$
$t_w=10^6$

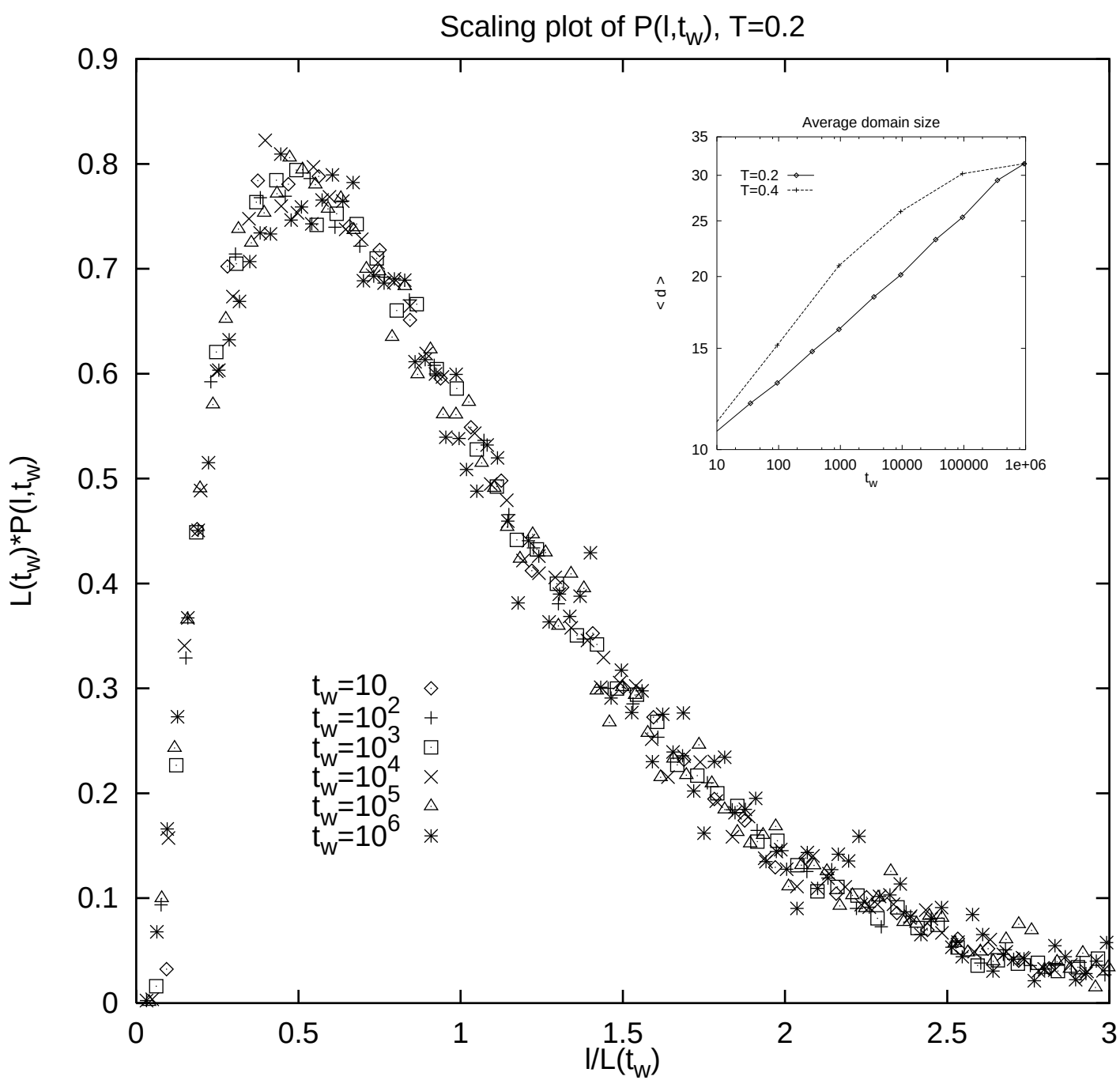
Scaling plot of P(l,t_w), T=0.2
L(t_w)*P(l,t_w)
l/L(t_w)
0
0.1
0.2
0.3
0.4
0.5
0.6
0.7
0.8
0.9
0
0.5
1
1.5
2
2.5
3
t_w=10
t_w=10^2
t_w=10^3
t_w=10^4
t_w=10^5
t_w=10^6
Average domain size
< d >
t_w
T=0.2
T=0.4
10
15
20
25
30
35
10
100
1000
10000
100000
1e+06

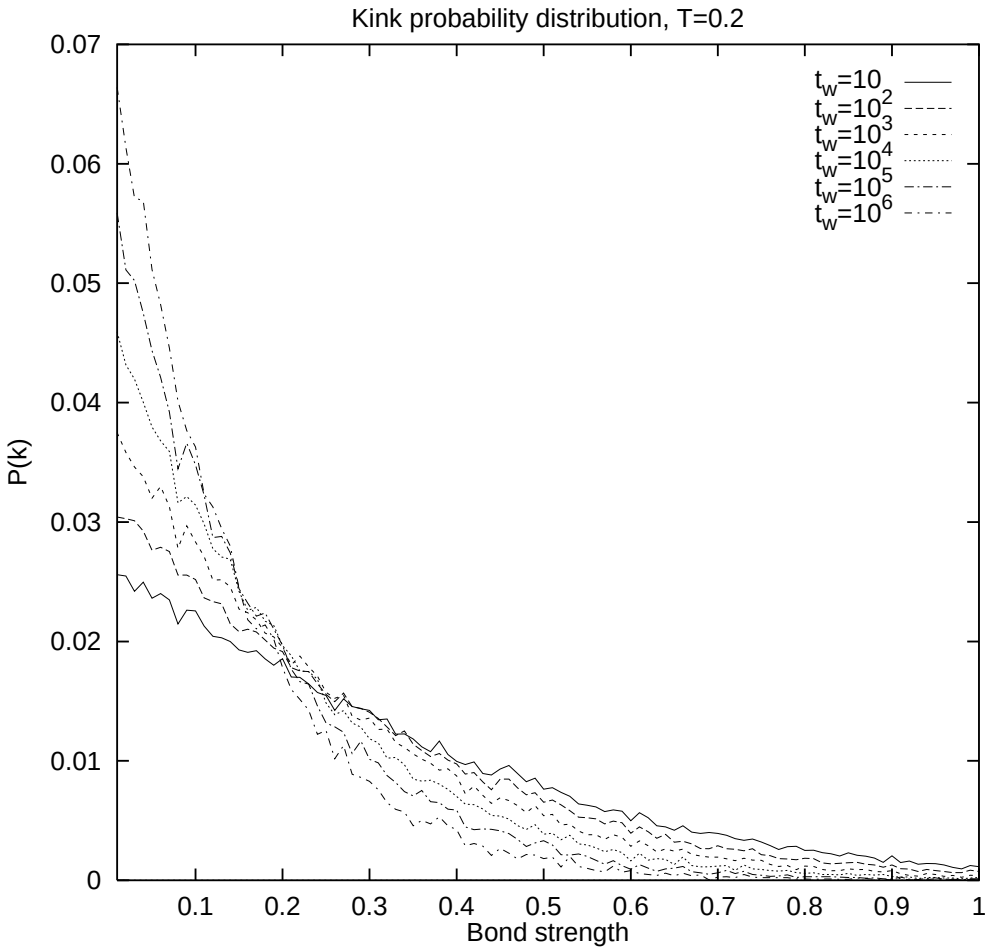
Kink probability distribution, T=0.2
P(k)
Bond strength
0.07
0.06
0.05
0.04
0.03
0.02
0.01
0
0.1
0.2
0.3
0.4
0.5
0.6
0.7
0.8
0.9
1
$t_w=10$
$t_w=10^2$
$t_w=10^3$
$t_w=10^4$
$t_w=10^5$
$t_w=10^6$

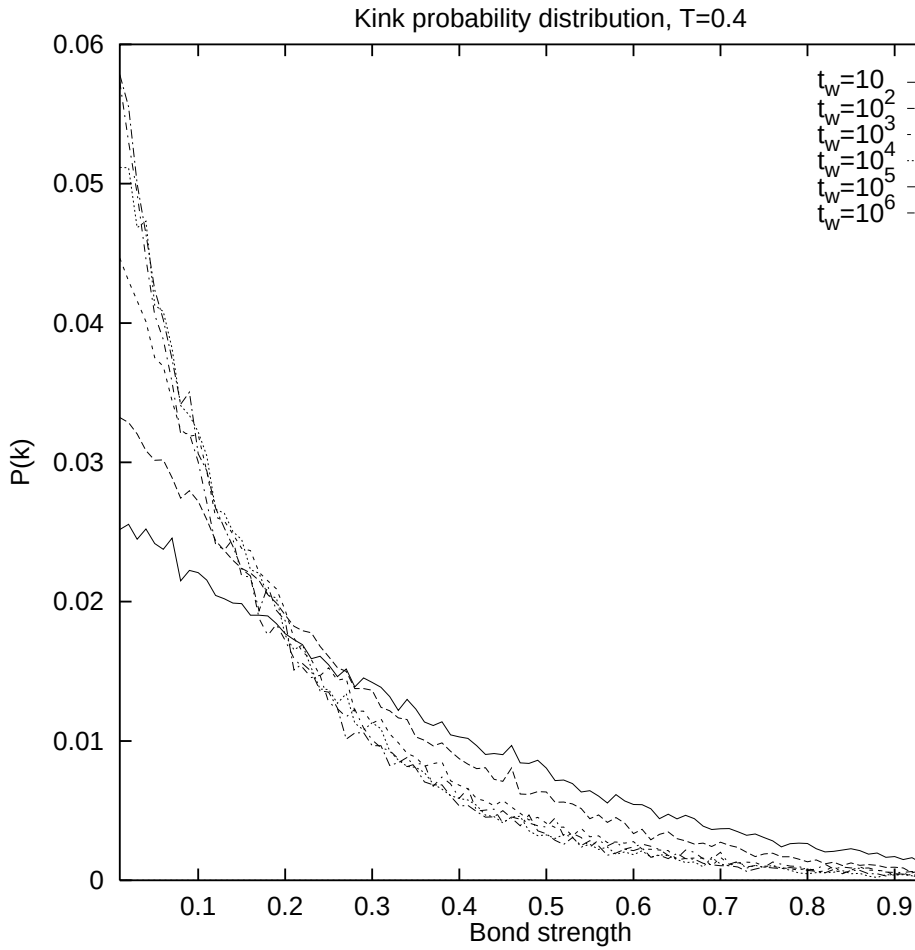
Kink probability distribution, T=0.4
P(k)
Bond strength
0.06
0.05
0.04
0.03
0.02
0.01
0
0.1
0.2
0.3
0.4
0.5
0.6
0.7
0.8
0.9
$t_w=10$
$t_w=10^2$
$t_w=10^3$
$t_w=10^4$
$t_w=10^5$
$t_w=10^6$

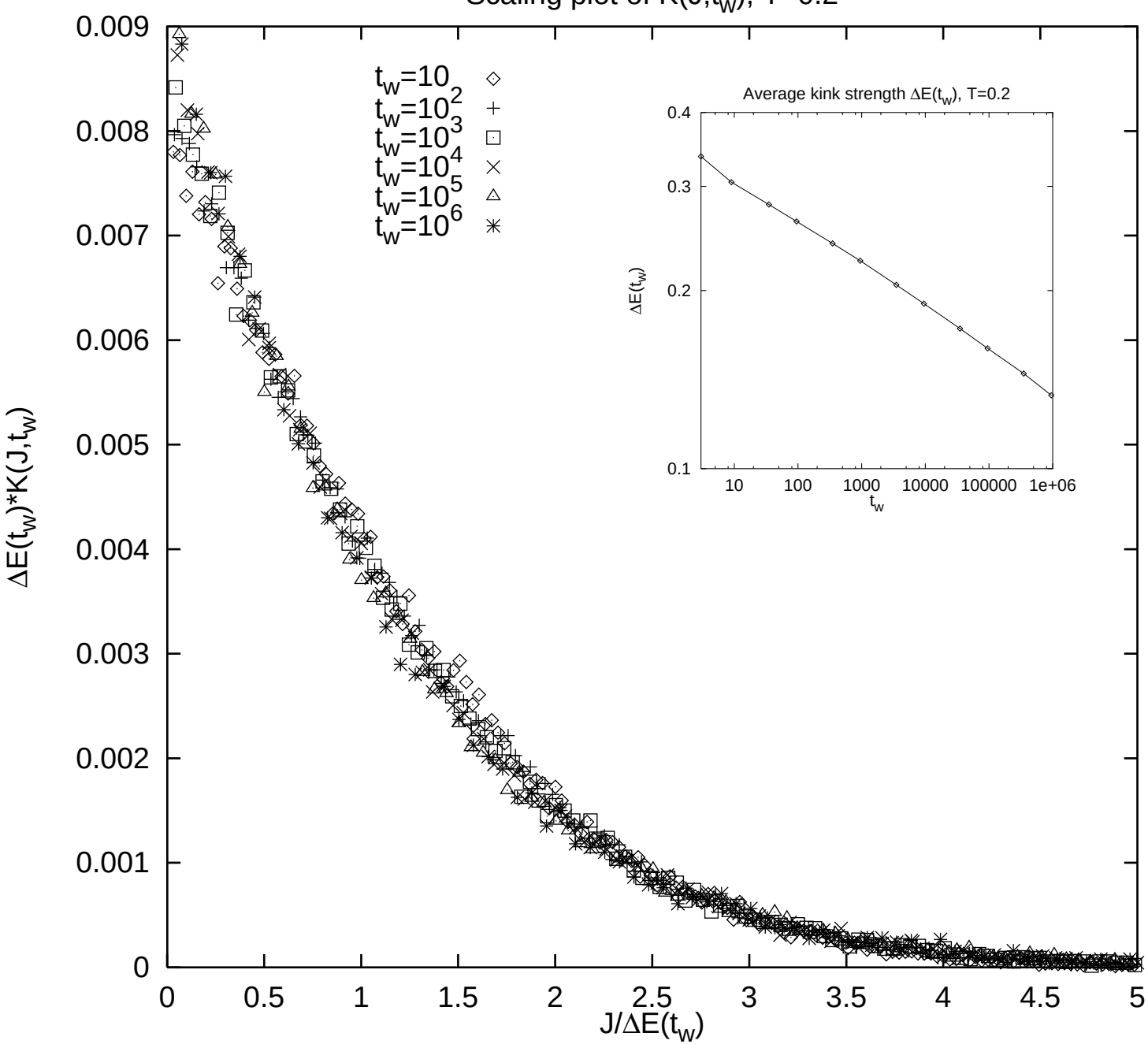
Scaling plot of K(J,t_w), T=0.2
ΔE(t_w)*K(J,t_w)
J/ΔE(t_w)
t_w=10
t_w=10^2
t_w=10^3
t_w=10^4
t_w=10^5
t_w=10^6
Average kink strength ΔE(t_w), T=0.2
ΔE(t_w)
t_w